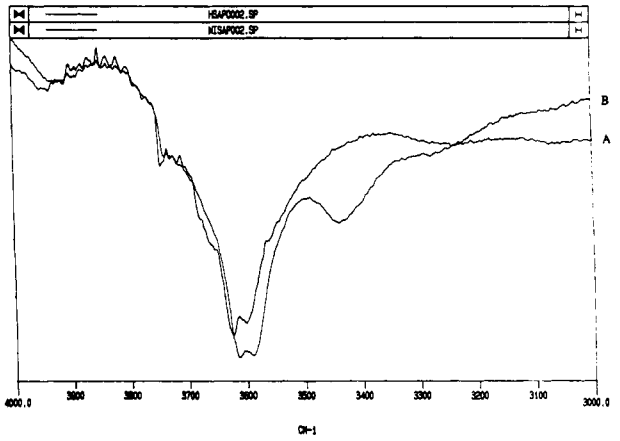

Figure 6. DRIFTS spectra of (A) calcined H-SAPO-34 and (B) Ni-SAPO-34.

subtleties of the mechanism of the catalytic reactions, doubtless arising from minor structural modifications of the active site. Finally, since the Li-NiSAPO34 again gave a similar EXAFS spectrum to that of the calcined Ni-SAPO34, this strongly indicates that the nickel cations cannot be present as exchangeable cations.

Diffuse reflectance infrared Fourier transform spectroscopy of calcined Ni-SAPO-34 shows the presence of a broad O-H stretching absorption band between 3490 and 3370 cm^{-1}, which is absent in the calcined SAPO-34 (Figure 6). We believe that this feature as well as the peaks at 3623 and 3597 cm^{-1} may be associated with Si-O(H)-Al Bronsted sites. Halik et al.[17] have assigned peaks close to 3623 and 3597 cm^{-1} to Bronsted acid sites of this kind in samples of SAPO similar to those used here. We are less clear of the origin of the broad peak centered around 3430 cm^{-1}. Adsorption of methanol at room temperature does not alter the broad feature. It is possible that there is a bridging hydrogen-bonded species present, which stabilizes the framework substitution of Ni in SAPO-34.

Since the O-H stretching bands of Ni-SAPO-34 are more intense than those of the H^+-SAPO-34, we conclude that the nickel-bearing catalyst has a higher density of acid sites. Its catalytic activity and selectivity is thus seen to be associated with the modification of the acidity of the zeolite by nickel and doubtless by subtle structural changes within the active site.

EXAFS analysis proves that the nickel is incorporated into the structure, with a large perturbation of the local environment. It also suggests the presence of a second extraframework coordination sphere, which from infrared spectroscopy seems to involve hydrogen bonding. This is postulated to stabilize the local structure around the nickel. We have, at present, no clear-cut evidence for the nickel having any direct role in the methanol conversion reaction, but it seems to modify the Bronsted acidity of the SAPO-34. Access to the nickel may be blocked by the bridging species observed by EXAFS and DRIFTS. Further investigations into the nature of the active site of this remarkable catalyst are underway.

Acknowledgment. We thank the Science and Engineering Research Council for its support and the British Council for a maintenance grant to Y.X. We also acknowledge the guidance and cooperation of Prof. G. N. Greaves and his colleagues at the SERC Daresbury Laboratory.

(17) Halik, C.; Lercher, J. A.; Meyer, H. *J. Chem. Soc., Faraday Trans. 1* **1988**, *84*, 4457.

Two Electronically Distinct Copper Sites in $La_{2-x}Sr_xCuO_{4-\delta}$ Compounds for $0.10 \leq x \leq 0.20$

Mark A. Kennard,[†,§] Yiqiao Song,[‡,§] Kenneth R. Poeppelmeier,[†,§,⊥] and W. P. Halperin*[,‡,§,⊥]

Department of Chemistry, Department of Physics and Astronomy, Materials Research Center, Science and Technology Center for Superconductivity, Northwestern University, Evanston, Illinois 60208

Received February 11, 1991. Revised Manuscript Received April 19, 1991

We report copper NQR and NMR measurements performed on the series $La_{2-x}Sr_xCuO_4$ ($0.10 \leq x \leq 0.20$). For each composition, two distinct sites of copper were observed. The relative occupation of the two sites correlates well with strontium doping. Transverse NMR shifts ($H \perp c$) of the two copper sites were derived from the NMR and NQR spectra. The temperature dependence of the ^{63}Cu NMR frequency shifts are identical for both sites, indicating that they have the same electronic spin susceptibility and hyperfine fields, and both are in the superconducting phase having the same critical temperature. However, these two sites have distinct orbital frequency shifts and electric field gradients.

Introduction

$La_{2-x}Sr_xCuO_{4-\delta}$ materials are structurally simpler than the other copper oxide superconductors. At room temperature, the superconducting members of this family have the tetragonal K_2NiF_4 structure space group $I4/mmm$-D_{4h}^{17} (ref 1) (see Figure 1) but convert to the orthorhombic structure $Abma$-D_{2h}^{18} (ref 2) by tilting of the oxygen octahedra below a transition temperature T_d. In both the

† Department of Chemistry.
‡ Department of Physics and Astronomy.
§ Materials Research Center.
⊥ Science and Technology Center for Superconductivity.

(1) Nguyen, N.; Choisnet, J.; Hervieu, M.; Raveau, B. *J. Solid State Chem.* **1981**, *39*, 120-127.
(2) Grande, V. B.; Müller-Buschbaum, Hk.; Schweizer, M. *Z. Anorg Allg. Chem.* **1977**, *428*, 120-124. Fleming, R. M.; Batlogg, B.; Cava, R. J.; Rietman, E. A. *Phys. Rev. B* **1987**, *35*, 7191.

0897-4756/91/2803-0672$02.50/0

Table I. Analytical and Structural Data of $La_{2-x}Sr_xCuO_{4-\delta}$ Compounds

composition		lattice parameters, Å			% Cu sites with			
x	δ	a	c	T_c, K	0-Sr	1-Sr	2-Sr	% site B Cu from NOR
0.10	−0.02 (3)	3.783 (3)	13.208 (19)	30.0	66	28	5	11
0.12	−0.01 (3)	3.781 (2)	13.227 (10)	31.8	61	31	7	11
0.16	−0.01 (3)	3.775 (4)	13.241 (15)	36.3	51	36	11	15
0.20	−0.02 (3)	3.772 (4)	13.250 (20)	28.4	43	38	15	20

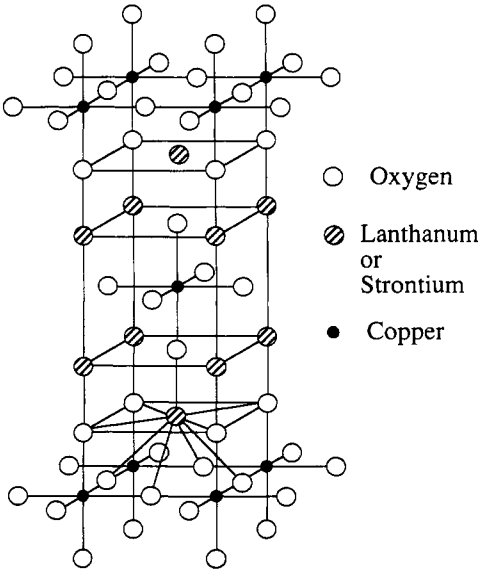

Figure 1. $La_{2-x}Sr_xCuO_{4-\delta}$ tetragonal structure, space group $I4/mmm$-D_{4h}^{17}. Copper is coordinated by oxygen in a distorted octahedral arrangement. This view highlights the perovskite substructure, where a cube of eight lanthanum/strontium sites surrounds the copper sites.

high-temperature tetragonal phase and the low-temperature orthorhombic phase there is only one site for copper atoms in the asymmetric unit.

When carefully prepared, superconducting $La_{2-x}Sr_xCuO_{4-\delta}$ compounds appear inherently homogeneous as measured by X-ray and neutron diffraction. Recently, Tan et al.,[3] claimed that $La_{2-x}Sr_xCuO_{4-\delta}$ compounds contain some five- as well as six-coordinated copper based on XANES results. In their model, some of the apical oxygen move to a tetrahedral interstitial site in the [LaO] layer. However, neither an apical oxygen vacancy nor an oxygen in an interstitial site is detected by diffraction at any temperature.[4] Using nuclear magnetic resonance and nuclear quadrupolar resonance techniques, which are sensitive to changes in the local electronic environment, we have determined that copper exists in two distinct environments and that both are intrinsic to the superconductor.

Experimental Section

$La_{2-x}Sr_xCuO_{4-\delta}$ compounds were synthesized by the solid-state reaction of 99.9999% pure La_2O_3 (Alpha) and CuO (Johnson & Mathey) and 99.995% pure $SrCO_3$ (Aldrich). Starting materials were dried, and their formula weights were confirmed by thermogravimetric analysis prior to use. The product phase formed after initial reaction at 950 °C for 2 days, as determined by X-ray powder diffraction. The samples were annealed in air at 950 °C for an additional 28 days with repeated grinding and pressing to ensure that the reaction had achieved equilibrium. The samples were quenched from high temperature after each heating to reduce the possibility of nucleation of $La_2SrCu_2O_6$. The products were protected from contamination by using a barrier pellet, which precluded direct contact with the container.

X-ray powder diffraction patterns of gound polycrystalline samples obtained by using a Rigaku Geigerflex diffractometer and a Cu Kα radiation source (λ = 1.541 78 Å) with a Ni filter. Typical scan parameters were $5 < 2\theta < 90°$, a slit width of 0.3° and a step width of 0.05°. Ground silicon single crystal pieces (Aldrich 99.9999% pure) were used as an internal standard. Peak positions and intensities were determined by fitting the data to a 50% mixture Gaussian and Lorentzian functions. The unit cell parameters shown in Table I were calculated by using the POLSQ[5] fitting program.

Thermogravimetric analysis, used to determine oxygen content, was obtained on a Du Pont thermal analysis system. Weight loss of a sample in a flow of 8.5% H_2/He gas was attributed to the reduction of all copper species to copper metal. All of the samples used in this study were oxygen stoichiometric ($\delta = 0.00 \pm 0.02$).

Magnetic susceptibility was measured with a Quantum Designs susceptometer, Model MPMS, calibrated with a platinum standard. Powders were contained in a gelatin capsule suspended in a clear straw. A small, diamagnetic, temperature independent subtraction was applied to correct for the sample holder. For T_c measurements, the samples were cooled in a nominally zero field. The field was increased to 1 mT, and then magnetization data were taken while increasing the temperature. The transition temperatures were determined by extrapolating a line from the region with the maximum slope to the temperature axis intercept. For normal-state measurements, a field of 1 T was used. Our results showed that $La_{1.84}Sr_{0.16}CuO_4$ has the highest T_c and the sharpest transition, which is consistent with other reports.[6]

Nuclear resonance spectra were obtained by using an alternate-phase, spin-echo pulse sequence of the form $\pi/2$, τ, π, where τ is the time between pulses. Typical parameters were $\pi/2 = 5$ μs, τ = 30–50 μs, and $\pi = 10$ μs. NQR experiments were performed on approximately 2 g of powder samples.

Aligned samples for NMR experiments were obtained by mixing finely ground powder samples with Emerson & Cumings STYCAST 1266 epoxy. The filling factor was about 15% by volume. The mixture was allowed to cure for 12 h in a 7.4-T magnetic field. Owing to magnetic anisotropy in the normal state, this procedure aligns the c axis of the grains in the direction of the magnetic field. The X-ray diffraction pattern of $La_{1.80}Sr_{0.20}CuO_4$ cast in epoxy showed an 8-fold increase in the relative intensity of (00l) diffraction peaks in comparison with the unaligned powder. Rocking curve measurements gave a peak width of 7.8° θ (full width at half-maximum), also indicating significant crystal alignment. Furthermore, both ^{63}Cu and ^{139}La NMR resonance frequencies were found to depend on the orientation of the sample alignment axes with respect to the applied magnetic field. Magnetic resonance measurements were performed on approximately 1.1 g of superconductor in the aligned samples at a magnetic field 3.4673 T.

Results

All of the compounds formed a solid solution with the tetragonal K_2NiF_4 structure. The crystallographic data, give in Table I, is in good agreement with those reported

(3) Tan, Z.; Filipkowski, M. E.; Budnick, J. I.; Heller, E. K.; Brewe, D. L.; Chamberland, B. L.; Bouldin, C. E.; Woicik, J. C.; Shi, D. *Phys Rev Lett* **1990**, *64*, 2715.

(4) Nguyen, N.; Choisnet, J.; Hervieu, M.; Raveau, B. *J. Solid State Chem.* **1981**, *39*, 120–127. Tarascon, M.; Greene, L. H.; McKinnon, W. R.; Hull, G. W.; Geballe, T. H. *Science* **1987**, *234*, 1373. Fleming, R. M.; Batloog, B.; Cava, R. J.; Rietman, E. A. *Phys. Rev. B* **1987**, *35*, 7191.

(5) Keszler, D.; Ibers, J. A. Modified POLSQ, Department of Chemistry, Northwestern University, 1983.

(6) Van Dover, R. B.; Cava, R. J.; Batlogg, B.; Rietman, E. A. *Phys Rev B* **1987**, *35*, 5337. Cheong, S. W.; Thompson, J. K.; Fisk, *Z. Physica C* **1989**, *158*, 109–126.

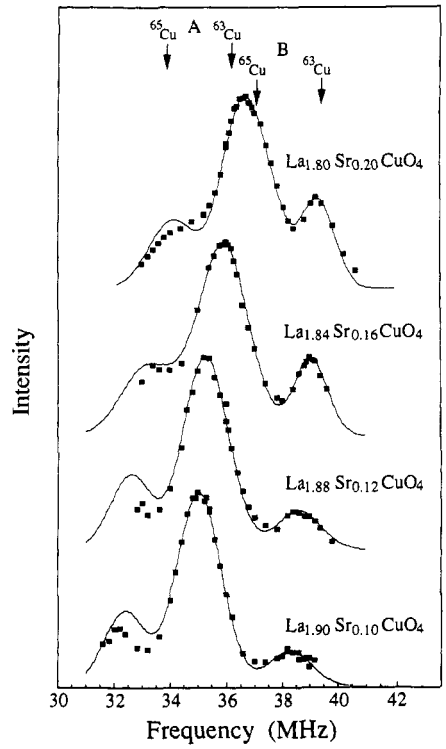

Figure 2. Copper NQR (H = 0) spectra of $La_{1.90}Sr_{0.10}CuO_4$, $La_{1.88}Sr_{0.12}CuO_4$, $La_{1.84}Sr_{0.16}CuO_4$, and $La_{1.80}Sr_{0.20}CuO_4$. Each spectrum shows three peaks indicating the presence of two electric field gradients for copper in the sample. The spectra were fit to Gaussian functions based on the presence of two copper sites A and B taking into account the different T_2 for each site. The peak near 39 MHz grows in intensity compared to the central peak, indicating that the mole fraction of that type of copper, designated site B in the text, increases with increasing strontium doping.

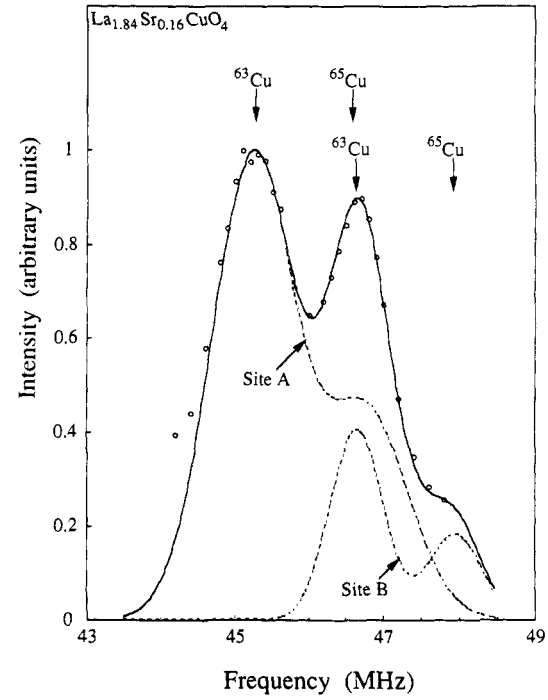

Figure 3. Copper NMR spectrum of $La_{1.84}Sr_{0.16}CuO_4$ at 5 K with the aligned axis perpendicular to the field ($H \perp c$). The deconvoluted spectrum shows that two copper sites are observed in the NMR as was observed in the NQR spectra in Figure 2. The mole fraction of site B determined from fitting the NMR matches that from the NQR within the error.

in the literature.[7] All observed diffraction peaks were indexable on the tetragonal cell of $La_{2-x}Sr_xCuO_{4-\delta}$. No diffraction peaks were observed from impurities, including $La_2SrCu_2O_6$.

The observed copper NQR spectra of $La_{1.90}Sr_{0.10}CuO_4$, $La_{1.88}Sr_{0.12}CuO_4$, $La_{1.84}Sr_{0.16}CuO_4$, and $La_{1.80}Sr_{0.20}CuO_4$ are shown in Figure 2. All spectra show three peaks, near 34, 36.5, and 39 MHz. As strontium doping is increased, the highest frequency peak grows in intensity relative to the other two, and the central peak appears to shift to higher frequency. Our spectra are in general agreement with those of Kumagai and Nakamura,[8] Ishida et al.,[9] and Yoshimura et al.[10] However it was Yoshimura et al.[10] that first noted two sets of resonance peaks in the NQR of related compounds.

A copper nucleus (with nuclear spin $I = {}^3/_2$) in a noncubic environment has only one allowed transition, between spin states $\pm{}^3/_2 \leftrightarrow \pm{}^1/_2$. The two isotopes of copper occur with relative abundance of $^{63}Cu/^{65}Cu = 2.235$, and the ratio of their quadrupolar moments, $^{63}Q/^{65}Q$, is 1.081. Thus a NQR spectrum of copper consists of pairs of peaks, one for each isotope in which the ratio of intensities is 2.235, and the ratio of the frequencies is 1.081. The three peaks in the NQR spectra indicate the presence of more than one electric field gradient for copper in the sample. Following this reasoning, the spectra were modeled by using two pairs of Gaussian functions, A and B, each pair scaled to the relative abundance and quadrupolar shift of $^{63}Cu/^{65}Cu$. The solid lines in Figure 2 were fit to each raw data set by varying the relative amount of copper A to copper B and adjusting the intensity for the spin–spin relaxation rate. In the experiment, the intensity observed for each resonance is proportional to $\exp(-2\tau/T_2)$, where τ is the delay time between the tipping pulse and the realignment pulse. Since the two sites have different spin–spin relaxation rates, the observed intensities are not in true proportion to their absolute amounts. Therefore, T_2 was measured at each peak for each compound, and a correction was applied in order to determine the true intensity. The mole fraction of each site as function of composition obtained from this analysis is listed in Table I. The mole fraction of site B increases with increasing strontium substitution, whereas the mole fraction of site A decreases with increasing strontium substitution.

Two peaks were observed in the NMR spectrum of $La_{1.84}Sr_{0.16}CuO_4$ at 5 K with $H \perp c$ (Figure 3). A good fit of the peaks was obtained based on the two-site model. For each pair of functions the intensity and frequency of the ^{65}Cu was scaled to that of ^{63}Cu. The deconvoluted spectrum shows that the intensity of the peak at 46.8 MHz is too large to be attributed to the ^{65}Cu associated with the ^{63}Cu resonance at 45.3 MHz, demonstrating that there are two inequivalent copper sites in the NMR spectrum as was observed in the NQR spectra. The relative amount of each type of copper site was found to be 21 ± 4%, quite close to that determined independently from the NQR fitting, 15 ± 3%. As with the NQR experiments, T_2 measured at the peak frequencies was used to correctly determine the intensities. One important distinction between the NQR and NMR analyses is that the symmetry and principle axis of the electric field gradient tensor plays an important role in determining the NMR spectrum but not the NQR spectrum. Agreement between B site occupancies deduced

(7) Tarascon, M.; Greene, L. H.; McKinnon, W. R.; Hull, G. W.; Geballe, T. H. *Science* **1987**, *234*, 1373.
(8) Kumagai, K.; Nakamura, Y.; *Physica C* **1989**, *157*, 307.
(9) Ishida, K.; Kondo, T.; Kitaoka, Y.; Asayama, K. *J. Phys. Soc. Jpn.* **1989**, *58*, 2638.
(10) Yoshimura, K.; Imai, T.; Shimizu, T.; Ueda, Y.; Kosuge, K.; Yasuoka, H. *J. Phys. Soc. Jpn.* **1989**, *58*, 9, 3057.

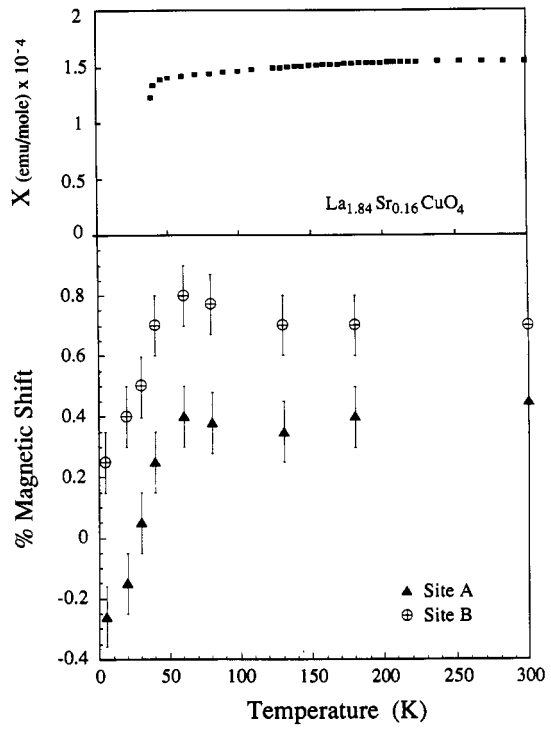

Figure 4. Magnetic shift and bulk magnetic susceptibility of $La_{1.84}Sr_{0.16}CuO_4$ as a function of temperature. The magnetic susceptibility was measured on lose powder in a 1-T field and was corrected for core diamagnetism.[11] No diamagnetic correction of the field in the superconducting state has been applied to the magnetic shift. Both site A and B drop off markedly in the superconducting state, indicating that both are in the superconductor and have the same T_c. Neither site has strong temperature dependence above T_c, as expected from the total susceptibility.

from our analysis of NMR and NQR spectra provides convincing evidence that the local symmetry at A and B sites is the same.

The total magnetic shift is a microscopic measurement of the susceptibility at the nucleus and thus can be used to describe changes in electronic properties at the copper site. Measurement of both NQR and NMR with the applied field perpendicular to the aligned axis allowed us to determine the magnetic shift, K. The NMR spectra were calculated by exactly solving Schrödinger's equation using the Hamiltonian

$$\mathcal{H} = \gamma H(1 + K)I_z + \nu_Q(3I_x^2 - I^2)/6$$

where γ the gyromagnetic ratio, and ν_Q is the observed NQR resonance frequency. Here we assume axial symmetry of the copper electric field gradient. This calculation was repeated, varying the value of K, until the observed spectra were fit as shown for example at 5 K in Figure 3. The temperature dependence of the magnetic shift was determined by measuring NMR and NQR at a number of temperatures between 5 and 300 K.

The magnetic shift is shown in Figure 4 as a function of temperature for $La_{1.84}Sr_{0.16}CuO_4$. For comparison, the total magnetic susceptibility, corrected for core diamagnetism,[11] is shown in the top portion of the figure. No Curie component was observed in the magnetic susceptibility of our sample. In the normal state, the total magnetic shift was temperature independent for both copper sites, in agreement with the temperature independent normal state susceptibility. Both types of copper, A and B, show a large decrease in shift below T_c. The decrease in the superconducting state is interpreted as a quenching of the spin susceptibility. This shift measurement demonstrates that both types of copper experience the same total spin susceptibility, and thus both are in the superconducting sample. Furthermore, the onset of the downturn in the shift occurs at the same temperature for both types of copper, indicating that they have the same T_c. Notably, neither the total susceptibility nor the shift shows features associated with the orthorhombic-to-tetragonal structural phase transition, T_d, near 180 K.

Below T_c, there is a reduction of the applied field associated with shielding currents of the superconducting electrons. Reduction of the field at the copper nucleus contributes to the total magnetic shift in the superconducting state. This diamagnetic frequency shift can be estimated by measuring the resonance of a spectator nucleus, in this case ^{139}La. This technique was recently demonstrated by Barrett et al.,[12] using ^{89}Y to obtain a corrected field at the copper nucleus in $YBa_2Cu_3O_7$. In our $La_{1.84}Sr_{0.16}CuO_4$ sample, the ^{139}La NMR peaks for the $^1/_2 \leftrightarrow {}^{-1}/_2$ and $^1/_2 \leftrightarrow {}^3/_2$ transitions were observed at 22.0 ± 0.05 MHz and 24.4 ± 0.1 MHz at 5 and 300 K. Thus, below T_c, the magnetic field in the sample is not significantly shifted. However the resolution of the peaks in the ^{139}La NMR was not adequate to determine the field to an accuracy better than 0.25%. Thus the shift values in Figure 4 are reported as measured and are not corrected for diamagnetism in the superconducting state. It is likely that the negative shift at 5 K for the A site copper can be attributed to diamagnetism. This correction would just shift both A and B curves up by the same amount in the superconducting state. Above T_c, no shielding correction is needed.

Discussion

From the resonance data of these $La_{2-x}Sr_xCuO_{4-\delta}$ compounds, it is clear that there are two types of copper sites, which we have designated site A and site B. Each has a distinct electric field gradient but the same T_c. We now discuss possible explanations of these results.

We first consider the possibility that site B corresponds to a second phase difficult to detect by diffraction. Recent neutron diffraction studies[13] of $La_{2-x}Sr_xCuO_{4-\delta}$ for x between 0.05 and 0.5 have shown that a miscibility gap exists for x between 0.20 and 0.50. All samples within the miscibility gap are a mixture of compounds with x corresponding to 0.20 and 0.50. We therefore report only results for doping levels between $x = 0.10$ and 0.20, where only one phase was detected by X-ray diffraction experiments.

On the basis of muon spin rotation experiments, Harshman et al.[14] argued that $La_{2-x}Sr_xCuO_{4-\delta}$ compounds form a mixture of superconducting and nonsuperconducting material for all compositions except that corresponding to the maximum in T_c ($x \approx 0.16$). If we were to ascribe site B to a second phase, then its mole fraction would be lowest at $x = 0.16$ and would increase as we move away from this composition. Clearly this behavior was not observed in the NQR spectra, where the intensity of site

(11) Selwood, P. W. *Magnetochemistry*; Interscience Publishers Inc.: New York, 1956; p78.

(12) Barrett, S. E.; Durand, D. J.; Pennington, C. H.; Slichter, C. P.; Friedmann, T. A.; Rice, J. P.; Ginsberg, D. M. *Phys. Rev. B* **1990**, *41*, 6283.

(13) Jorgensen, J. D.; Lightfoot, P.; Pei, S.; Dabrowski, B.; Richards, D. R.; Hinks, D. G. Invited paper to the Third International Symposium on Superconductivity, Sendai, Japan, Nov 1990. To be published by Springer-Verlag, Tokyo.

(14) Harshman, D. R.; Aeppli, G.; Batlogg, B.; Espinosa, G. P.; Cava, R. J.; Copper, A. S.; Rupp, L. W.; Ansaldo, E. J.; Williams, D. L. *Phys. Rev. Lett.* **1989**, *63*, 1187.

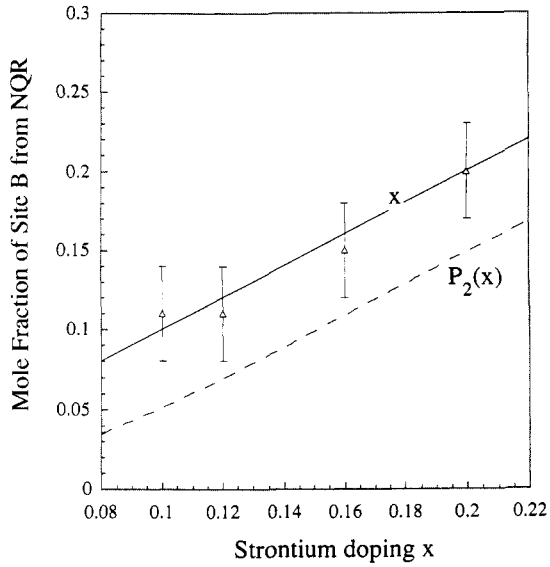

Figure 5. Compositional dependence of the mole fraction of the second type of copper. The mole fraction of site B increases with increasing strontium doping. The solid line is the strontium doping x. The dashed line is the probability of two strontium atoms randomly occupying one of the eight lanthanum sites in the second coordination sphere of copper calculated as a function of doping, $P_2(x)$.

B increases monatonically with increasing strontium doping as shown in Figure 5. Our transverse NMR shift measurements (see Figure 4) demonstrate that site B undergoes the same decrease in the spin susceptibility as site A, implying that it has the same hyperfine contact with the conduction electrons which pair below T_c. The copper nuclei corresponding to site B must be in the same superconducting phase as those of site A, since the temperature dependence of the transverse NMR frequency shift is identical for both sites. In summary, we see no evidence in our spectra for a second phase.

Next we consider the compositional dependence of the mole fraction of this second type of copper. One possible explanation is that strontium substitution for lanthanum causes a shift in the resonance frequency of some of the copper either by distortion of its electric field or by inducing bonding or coordination changes. In the K_2NiF_4 structure (see Figure 1) copper atoms are surrounded by eight next-nearest-neighbor lanthanum or strontium atoms in roughly a cubic geometry. For each composition there is a distribution of the occupancy of these eight sites. The probability of finding zero (P_0), one (P_1), or two (P_2) strontium atoms in the eight sites was calculated from the distribution function

$$P_n(x) = (x/2)^n(1 - x/2)^{N-n}N!/n!(N - n)!$$

This calculation ignores the effect of the arrangement of strontium atoms around the copper atoms. They may be located on the cube's body diagonal, face diagonal, or adjacent to one another. The occupancy distribution of these sites for each doping level of strontium is given in Table I. If we only consider the occupancy of 0-Sr and 1-Sr (zero or one strontium in the second coordination sphere), this model predicts four peaks with a ratio of P_0, $2.23P_0$, P_1, and $2.23P_1$. The calculated mole fraction for site B based on one strontium atom affecting every adjacent copper atom is approximately twice as large as is observed. For example, consider $La_{1.84}Sr_{0.16}CuO_4$ where the calcultaed mole fraction of 1-Sr is 36%, compared to the observed value of 15 ± 3%. Thus the perturbing effect on the electric field gradient of copper atoms by placing one divalent strontium in the second coordination sphere of copper cannot account for the observed ratio of sites A and B.

The mole fraction of site B does have a reasonable correlation to the probability of two strontium atoms in the second coordination sphere of some of the copper, P_2, if the mole fraction of site A is attributed to the balance, [A] = 1 - [B]. One possible explanation[15] for this correlation is based on an oxygen defect model, proposed by Tan et al.[3] They hypothesized that strontium atoms adjacent to each other in the second coordination sphere of copper induce an apical oxygen to migrate to the tetrahedral interstitial site of four neighboring lanthanum atoms. In their model, movement of the apical oxygen produces five-coordinated copper, which one might assign to site B in the NQR. However, it is known from earlier work[16] that A_2BO_4-related materials lose oxygen from the planar site more easily than from the apical position. It is also specifically known that oxygen is lost from the plane sites in $La_{2-x}Sr_xCuO_{4-\delta}$ for x larger than 0.25.[1,17] Most importantly, neutron diffraction studies[18] do not support occupation of the interstitial site by oxygen or the formation of five-coordinate copper.

The difference between the total magnetic shift of site A and B is nearly constant at all temperatures. This difference, 0.4 ± 0.1% is attributed to the orbital contribution to the shift of site B relative to site A. To obtain a difference in orbital shifts of the magnitude observed, it is necessary that a large difference in either coordination or oxidation state must exist between the two sites. If the substitution of two strontium atoms into the second coordination sphere of copper causes local distortion of the copper oxygen bonds, the distortion must be consistant with the average structure.

We can further constrain possible models for site B based on the NMR spectrum (Figure 3). The copper atoms corresponding to site A have uniaxial symmetry along c axis of the crystal structure. Since the material is magnetically anisotropic, we can align this unique axis of the site A copper with respect to an applied field and then maintain this configuration with an epoxy resin. This gives rise to narrowing of the resonance line in the aligned crystallites. However, the a and b axes are randomly distributed because they are equivalent in the tetragonal structure at room temperature. Thus the fact that the NMR peak frequency for site B is as narrow as the peak for site A suggests that site B has the same symmetry. This argues against the B site arising from the displacement of one of the planar oxygen atoms surrounding copper.

Another possible explanation is that the copper nuclei that give rise to site B have a higher oxidation level than those that correspond to site A.[10] Each strontium formally causes the oxidation of one copper, so that the mole fraction of site B in this case would scale as the amount of strontium doping. Copper atoms in the vicinity of strontium are more likely to achieve a higher oxidation level resulting in defect pairing. This localization of charge must still allow for delocalized conduction electron character, as indicated by the identical downturn of the copper

(15) Yoshimura, K.; Kosuge, K.; Imai, T.; Shimizu, T.; Yasuoka, H. Preprint.
(16) Leonowicz, M. E.; Poeppelmeier, K. R.; Longo, J. M. *J. Solid State Chem.* **1985**, *59*, 71.
(17) Soderholm, L.; Capone, D. W.; Hinks, D. G.; Jorgensen, J. D.; Schuller, I. K. *Inorg. Chim. Acta* **1987**, *140*, 167.
(18) Kwei, G. H.; Partin, D. E. *Phys. Rev. Lett.* **1990**, *65*, 3456. Jorgensen, J. D.; et al. Argonne National Laboratory, Argonne, IL 60439, unpublished.

shift at site A and B below T_c in Figure 4.

Figure 5 shows a plot of the mole fraction of site B from Cu NQR intensity versus strontium doping. Of course the plot for site A is just the inverse since we defined the mole fraction of A as 1-B. The dashed line represents the calculated probability of 2-Sr in the second coordination sphere of copper, $P_2(x)$, from Table I. The mole fraction of site B calculated from the $P_2(x)$ is significantly less than observed. However, the probability distributions were calculated assuming random distribution of strontium atoms over all lanthanum sites. A model that includes attractive interactions, which could reflect a tendency of strontium atoms to cluster together, might achieve better agreement. The solid line is the value of strontium doping x, or the mole fraction of copper formally oxidized as a result of that doping. Interestingly, the observed mole fraction of site B correlates well with strontium substitution. We cannot distinguish between either model based solely on measured occupancies of the two sites.

Summary

We have demonstrated that the concentration of a second type of copper in the $La_{2-x}Sr_xCuO_{4-\delta}$ superconductor increases with increasing doping level. The magnetic shifts of both types of copper appear to be temperature independent in the normal state but have a steep drop below T_c. It is concluded from the similarity of their shift behavior (they have the same T_c) that both copper sites are located in the superconducting ($CuO_{4/2}$) plane. The existence of two microscopically distinct copper sites in this superconducting compound is unexpected considering the crystallographic structure.

Acknowledgment. This work was supported by the NSF-MRL program through the Northwestern Materials Research Center (Grant DMR-8821571). The Quantum Designs Magnetic Susceptometer was purchased by the NSF-STC program for superconductivity (Grant DMR-8809854).

Chemical Vapor Deposition of Platinum: New Precursors and Their Properties

Neil H. Dryden, Ravi Kumar, Eric Ou, Mehdi Rashidi, Sujit Roy, Peter R. Norton, and Richard J. Puddephatt*

Department of Chemistry, University of Western Ontario, London, Ontario, Canada N6A 5B7

John D. Scott

3M Canada Inc., C.P. Box 5757, London, Ontario, Canada N6A 4T1

Received February 14, 1991. Revised Manuscript Received May 14, 1991

The complexes *cis*-[PtMeRL$_2$], where R = Me, CH_2=CH, CH_2=$CHCH_2$, *t*-BuC≡C and L = MeNC or L_2 = 1,5-cyclooctadiene, are shown to be useful precursors for the chemical vapor deposition (CVD) of platinum films under mild conditions. Carbon impurities in the films and the temperature of CVD were both greatly reduced when CVD was carried out in the presence of hydrogen, but CVD was retarded in the presence of free MeNC. The σ-allylplatinum or σ-vinylplatinum complexes gave CVD at the lowest temperature. Thermolysis of *cis*-[$PtMe_2(MeNC)_2$] gives methane as a gaseous product, and this is shown to be formed by combination of a methylplatinum group with a hydrogen atom from H_2, if present, or from the cell wall. The carbon impurities in the platinum films formed by CVD in the absence of hydrogen were shown to be derived at least partly from the methylplatinum groups.

Introduction

Organometallic chemical vapor deposition (OMCVD) of thin-film metallic conductors has emerged as a useful technique for the fabrication of microelectronic components.[1,2] Recent studies[1b,3] in the OMCVD of III–V semiconductor materials have established that an understanding at the molecular level of the various chemical processes involved during the decomposition of the precursor is mandatory in controlling the growth and properties of the deposited semiconductor film. However, mechanistic studies have been few,[1b,4] and challenges remain in the detailed analysis of the various decomposition pathways, including separation of gas-phase and surface reactions, and in the kinetic modeling of CVD. There is a clear need for a better understanding of the fundamental

(1) (a) Sherman, A. *Chemical Vapor Deposition for Microelectronics: Principles, Technology, and Applications*; Noyes Publications: Park Ridge, New Jersey, 1987. (b) Gross, M. E., Jasinki, J. M., Yates, J. T., Eds. Chemical Perspectives of Microelectronic Materials. *Mater. Res. Soc. Symp. Proc.* **1989**, *131*. (c) Williams, J. O. *Angew. Chem., Int. Ed. Engl. Adv. Mater.* **1989**, *28*, 1110.

(2) (a) Jasinski, J. M.; Meyerson, B. S.; Scott, B. A. *Annu. Rev. Phys. Chem.* **1987**, *38*, 109. (b) Cole-Hamilton, D. J., Williams, J. O., Eds. *Mechanisms of Reactions of Organometallic Compounds with Surfaces*; NATO ASI Series B, 1989; Vol. 198.

(3) (a) Lee, P. W.; Omstead, T. R.; McKenna, D. R.; Jenson, K. F. *J. Cryst. Growth*, **1987**, *85*, 165. (b) Tsuda, M.; Oikawa, S.; Morishita, M.; Mashita, M. *Jpn. J. Appl. Phys.* **1987**, *26*, 6564.

(4) (a) Konstantinov, L.; Nowak, R.; Hess, P. *Appl. Phys.* **1988**, *A47*, 171. (b) Wood, J. *Vacuum* **1988**, *38*, 683. (c) Bent, B. E.; Nuzzo, R. G.; Dubois, L. H. *J. Am. Chem. Soc.* **1989**, *111*, 1634. (d) Speare, K. E.; Drix, R. R. *Pure Appl. Chem.* **1990**, *62*, 89. (e) Girolami, G. S.; Jensen, J. A.; Pollina, D. M.; Williams, W. S.; Kaloyeros, A. E.; Allocca, C. M. *J. Am. Chem. Soc.* **1987**, *109*, 1579. (f) Feurer, R.; Larhrafi, M.; Morancho, R.; Calsou, R. *Thin Solid Films* **1988**, *167*, 195. (g) Gladfelter, W. L.; Boyd, D. C.; Jensen, K. F. *Chem. Mater.* **1989**, *1*, 339. (h) Girolami, G. S.; Jeffries, P. M. *Chem. Mater.* **1989**, *1*, 8. (i) Sauls, F. C.; Interrante, L. V.; Jiang, Z. P. *Inorg. Chem.* **1990**, *29*, 2989.

0897-4756/91/2803-0677$02.50/0